



Underwater Explosion Performance of RDX/AP-based Aluminized Explosives

Dalin Xiang, Jili Rong,* Xuan He, Zhiwei Feng

*School of Aerospace Engineering, Beijing Institute of Technology,
Beijing, 100081, P. R. China*

**E-mail: rongjili@bit.edu.cn*

Abstract: To understand the underwater explosion (UNDEX) performance of RDX/AP-based aluminized explosives, six formulations of the explosives were prepared, with Al content varying from 30% to 55% and ammonium perchlorate (AP) content from 45% to 20%. A series of UNDEX tests that used a 1 kg cylindrical charge was conducted underwater at a depth of 4.7 m. The pressure histories of the shock wave produced at different positions and the bubble periods were measured. The coefficients of the similarity law equation for the shock wave parameters were fitted with experimental data. The effect of the aluminum/oxygen (Al/O) ratio on the performance of the energy output structure for RDX/AP-based aluminized explosives is discussed. The bubble motion during UNDEX was simulated using MSC.DYTRAN software, and the radius-time curves of the bubbles were determined. The results show that AP influences the detonation reaction mechanism of RDX/AP-based aluminized explosives, which causes different UNDEX performances. The bubble energy of the RDX/AP-based aluminized explosive was higher than that of RDX-based and HMX-based aluminized explosives.

Keywords: UNDEX, RDX/AP-based aluminized explosives, detonation, shock wave, Al/O ratio

1 Introduction

The underwater explosion (UNDEX) performance of explosives has been a concern for scholars and weapon designers. UNDEX parameters such as the peak pressure of the shock wave, bubble period, attenuation time constant, shock wave impulse, energy, and energy flux density, reflect the effectiveness of explosives [1]. The output and distribution of the forms of energy of aluminized explosives

reacting underwater are the major indices considered when evaluating the output performance and application range of explosives. The UNDEX performance is key in weapon design and target damage effects for military explosives.

Given their high combustion enthalpy, aluminum (Al) particles are widely used as additives in explosives to reduce the decay of the shock wave pressure, to increase the bubble energy in underwater weapons, and to influence the underwater warhead performance [2]. TNT, RDX and HMX are usually employed as matrix explosives, especially in underwater weapon warheads. In addition, ammonium perchlorate (NH_4ClO_4 , AP) is often added to aluminized explosives as an oxidant to enhance the oxidizability of the detonation products. Therefore, an understanding of UNDEX performance and energy distribution for different formulations of aluminized explosives containing AP is crucial for improving the design and widening the application of explosive formulations.

Previous studies have investigated the effects of formulation composition on the detonation performance and on the prediction of detonation parameters for aluminized explosives [3-8]. However, systematic studies relevant to the UNDEX performance of aluminized explosives are few, especially UNDEX experiments that involve different formulations of explosives. The US Office of Naval Research summarized the characteristics of the transition from chemical energy to shock wave energy, analyzed the influence of different formulations on the energy output structure, and established a set of formulas to calculate the shock wave and bubble energy [9]. Swisdak *et al.* conducted experiments to analyze the variations in shock wave energy and bubble energy with changes in the Al/O ratio in TNT/RDX/Al formulations [10]. This study showed that shock wave energy initially increases with an increase in the Al/O ratio, reaches a maximum at an Al/O ratio of 0.4, and then gradually decreases, whereas the bubble energy increases continuously. Stromsoe and Eriksen observed the same trend in RDX/Al explosives after performing a set of UNDEX experiments [11]. Kumar *et al.* prepared some aluminized plastic-bonded explosive formulations that contained RDX, Al (0% to 35%), and HTPB, and evaluated their corresponding underwater performances. Explosion bulge tests were conducted for each explosive formulation, and the extent of the bulge in the test plates was presented and compared with that from a standard underwater explosive [12]. Wang *et al.* studied the effect of key factors on the energy output of emulsion explosives during UNDEX [13]. However, insufficient studies are available on RDX/AP-based aluminized explosives. Bocketeiner investigated the UNDEX performance properties of Australian-made PBX-115 (43/25/20/12 AP/Al/RDX/HTPB) and pointed out that PBW-115 should be a superior fill for use in underwater blast weapons [14]. Lu *et al.* simulated the detonation

and conducted the mid-scale underwater test of PBXW-115 [15]. They found that the detonation velocity and critical diameter are sensitive to the assumed AP decomposition rate.

Experimental evidence has demonstrated the effect of the Al particles on the detonation properties of some aluminized explosives, but the UNDEX performance cannot be quantitatively assessed in the absence of an appropriate experimental strategy for RDX/AP-based aluminized explosives. The present study aimed to investigate the energy output of RDX/AP-based aluminized explosives of various formulations by conducting UNDEX tests. This study provides a theoretical guide for the design of RDX/AP-based aluminized explosives by recognizing the energy release rule, controlling the break process, increasing the energy efficiency, and improving blast effects.

2 Explosive Specimens

The RDX/AP-based aluminized explosives employed in this study were all matrix explosives containing Al particles, wax, and graphite. The detailed formulations and detonation parameters of the aluminized explosives are shown in Table 1. Wax was immersed in ethyl acetate and heated to 50 °C for dissolution. RDX, AP, Al particles, and graphite were then added. The mixture was continuously heated and stirred until nearly all of the ethyl acetate had evaporated. The Al/O ratio refers to the mole ratio of Al and O for the average molecular formula of the aluminized explosive. The Al particles mixed in the explosives were granular. Each particle had a diameter of approximately 13 μm . The Al particles were not subjected to any pre-oxidation treatment and were evenly distributed in the mixed explosives. All of the cylindrical explosive specimens were prepared using a vacuum pouring process. The values of D , P_{CJ} and Q_v are the average of duplicate test results in accordance with the Chinese Military Standard (GJB772A-97).

Table 1. Formulations of the RDX/AP-based aluminized explosives

No.	Al/O	Proportion [wt.%]					ρ [g·cm ⁻³]	P_{CJ} [GPa]	D [m·s ⁻¹]	Q_v [kJ·kg ⁻¹]
		RDX	Al	AP	Wax	Graphite				
1	0.536	20	30	45	3	2	1.959	12.61	6020	8774.4
2	0.684	20	35	40	3	2	1.992	13.68	6097	8684.8
3	0.855	20	40	35	3	2	2.015	13.83	6176	8441.1
4	1.071	20	45	30	3	2	2.041	14.04	6247	8054.2
5	1.331	20	50	25	3	2	2.072	14.26	6344	7265.7
6	1.672	20	55	20	3	2	2.103	14.44	6400	6478.1

3 Experimental Method

3.1 Experimental conditions

The pool should be of adequate size to minimize the influence of the water surface, the side walls, and the bottom of the pool during UNDEX. A pool with a diameter of at least six times the maximum radius of the bubble was adopted in these experiments. The distance from the bottom to the charge should be more than twice the maximum radius of the bubble when the charge is placed at about two-thirds the depth of the pool [16, 17]. The calculation formula for the maximum bubble radius (r_{\max}) as given by Cole [1] is expressed as:

$$r_{\max} = \left(\frac{3Q}{4\pi P_H} \right)^{1/3} \quad (1)$$

where Q is the detonation products' surplus energy after the shock wave (J), and P_H is the hydrostatic pressure at the charge (Pa). The formula $Q = 0.41 W Q_v$ is also used, where W is the mass of the charge (kg), and Q_v is the detonation heat of the explosive (J/kg).

3.2 Experimental arrangement

Six experiments were conducted to investigate the UNDEX performance of the RDX/AP-based aluminized explosives, a schematic diagram of which is presented in Figure 1a. The experiments were conducted in a cylindrical water pool with a diameter of 85.0 m and a depth of 14.5 m. Six 1 kg cylindrical charges of the RDX/AP-based aluminized explosives were detonated in tap water at a depth of 4.7 m. Ten sensors were placed at 1.0 m, 1.5 m, 2.0 m, 2.5 m, and 3.0 m from the center of the explosive and facing the shock front. The length l and diameter d of the cylindrical charges ranged from 79.62 mm to 86.64 mm. The l/d ratios ranged from 1:1 to 1.2:1. The main charges were initiated by an initiation chain, which consisted of a no. 8 electric detonator and a 1:1 right cylindrical pressed JH-14 booster (*i.e.* 96.5% RDX and 3.5% fluororubber and graphite, by mass) of 10 g, as shown in Figure 1b. The density and detonation velocity of the JH-14 booster were 1.738 g/cm³ and 8428 m/s, respectively.

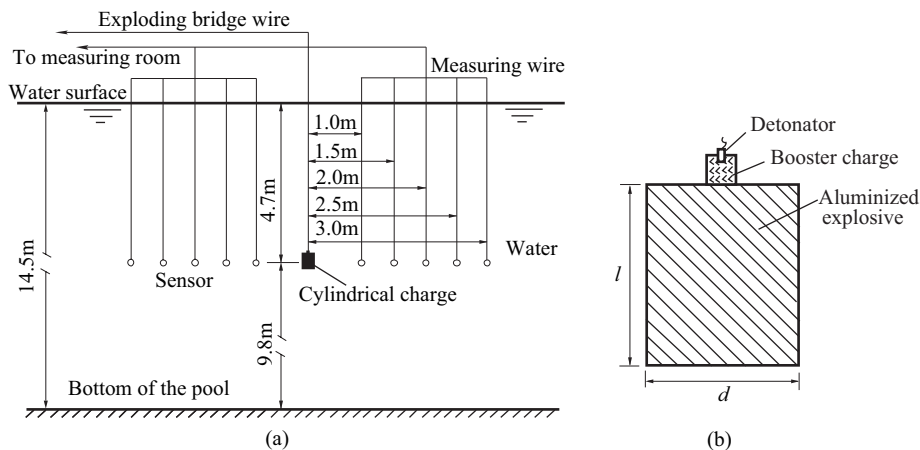


Figure 1. Sketch of the UNDEX experimental arrangement

4 Results and Discussion

4.1 Typical shock wave pressure history

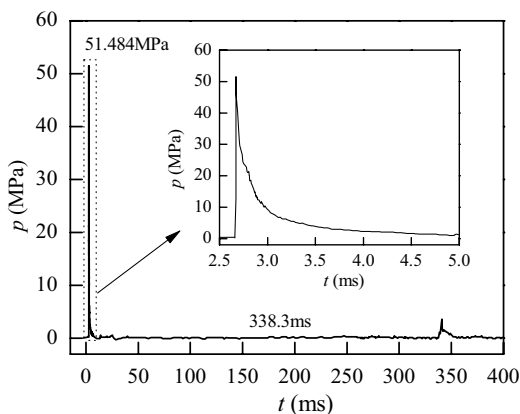


Figure 2. Typical pressure-time profile of a 1.0 kg explosive charge of Formulation 1 at 1.0 m. The graph insert shows a magnified version of the highlighted peak.

Figure 2 shows the shock wave and the bubble pulse at 1 m from Formulation 1 during the UNDEX recorded pressure-time history by the corresponding sensor (*i.e.* 400 ms pressure history and within 5.0 ms in the graph insert). The incident

shock wave arrived at 2.7 ms, with a peak value of 51.484 MPa, and had decayed rapidly by approximately 3.5 ms. The shock wave propagated with a broader profile and a lower maximum pressure, and the first bubble pulse appeared after approximately 338.2 ms. Thus, the bubble pulse period was 338.3 ms.

4.2 Detailed test results

Table 2 shows the detailed results of the experiments on different formulations of the RDX/AP-based aluminized explosives. The values in the table are the average values measured at the same measuring distances. R denotes the distance between the charge center and the measuring point (m), p_m represents the peak pressure of the shock wave (Pa), T_b refers to the period of the bubble (s), θ denotes the attenuation time constant (μs). θ is the time required by the peak pressure p_m to fall to p_m/e , where $e = 2.718$. The shock wave impulse I , shock wave energy E_s , shock wave energy flux density E , and the bubble energy E_b were calculated as follows [1]:

$$I(t) = \int_0^{6.7\theta} p(t) dt \quad (2)$$

$$E_s = \frac{4\pi R^2}{\rho_w C_w} \int_0^{6.7\theta} p^2(t) dt \quad (3)$$

$$E = \frac{1}{\rho_w C_w} (1 - 2.422 \times 10^{-4} p_m - 1.031 \times 10^{-8} p_m^2) \int_0^{6.7\theta} p^2(t) dt \quad (4)$$

$$E_b = 0.684 P_H^{5/2} T_b^3 / \rho_w^{3/2} \quad (5)$$

where $p(t)$ is the shock wave pressure (Pa), ρ_w is the water density (kg/m^3), C_w is the velocity of sound in water (1450 m/s), and p_m is the peak pressure of the shock wave (MPa).

Table 2. Results of the UNDEX experiments on the RDX/AP-based aluminized explosives

Al/O	R [m]	p_m [MPa]	T_b [ms]	E_s [MJ·kg ⁻¹]	E_b [MJ·kg ⁻¹]	E [MJ·m ⁻²]	I [kPa·s ⁻¹]	θ [μs]
0.536	1.0	51.484	338.3	1.665	6.328	0.13084	9554.0	142.32
	1.5	34.736		1.585		0.05559	6454.0	149.43
	2.0	24.888		1.512		0.02990	4767.8	155.52
	2.5	19.73		1.400		0.01774	3642.2	157.22
	3.0	17.311		1.316		0.01159	3298.5	163.43
0.684	1.0	50.620	340.9	1.558	6.483	0.12246	9367.5	136.56
	1.5	34.272		1.493		0.05237	6320.2	144.82
	2.0	23.846		1.408		0.02785	4620.2	146.78
	2.5	19.279		1.308		0.01658	3573.2	151.83
	3.0	16.832		1.204		0.01060	3198.3	157.77
0.855	1.0	47.95	339.7	1.441	6.414	0.11334	8777.2	130.85
	1.5	32.541		1.325		0.04649	5964.5	139.80
	2.0	22.819		1.257		0.02487	4370.6	143.54
	2.5	18.513		1.161		0.01472	3386.1	147.83
	3.0	15.789		1.073		0.00945	3052.8	155.15
1.071	1.0	46.471	335.7	1.315	6.189	0.10346	8114.6	117.83
	1.5	31.416		1.147		0.04026	5559.4	129.21
	2.0	21.621		1.101		0.02179	4106.0	138.43
	2.5	17.512		1.030		0.01306	3235.2	145.77
	3.0	15.304		0.998		0.00879	2880.6	151.50
1.331	1.0	43.795	332.0	1.098	5.976	0.08645	7693.3	112.34
	1.5	29.659		1.018		0.03575	5266.0	123.87
	2.0	20.606		0.972		0.01924	3847.2	135.14
	2.5	16.218		0.889		0.01127	2984.9	144.29
	3.0	14.648		0.811		0.00715	2719.1	147.33
1.672	1.0	41.419	324.1	0.897	5.544	0.07066	7189.1	102.74
	1.5	28.227		0.842		0.02958	4870.3	116.63
	2.0	19.211		0.751		0.01487	3576.5	123.63
	2.5	15.606		0.744		0.00944	2712.4	135.50
	3.0	13.826		0.701		0.00618	2496.0	141.85

Table 2 shows that while the component proportion of the matrix explosive RDX was maintained at 20%, the Al/O ratio was increased from 0.536 to 1.672. Moreover, p_m , E_s , E , I and θ at the same measuring point decreased incrementally for the different formulations, with average decreases of 20, 47, 47, 25, and 19%,

respectively, compared with that of Formula 1. However, changes in T_b and E_b are not apparent. T_b and E_b reached their maximum values when the Al/O ratio was 0.684. The high bubble energy can be associated with the detonation heat. A high detonation heat results in a high bubble energy, as previously demonstrated in RDX- and HMX-based aluminized explosives [18, 19]. However, the RDX/AP-based aluminized explosives do not follow this principle. AP has a low explosive energy (about 1112 J/g) and would not release more energy during explosive detonation. The apparent lack of changes in T_b and E_b can be explained by the effects of AP as an oxygen-rich additive. The detonation heat of RDX/AP-based aluminized explosives is considerably different. However, the bubble energy is almost unchanged.

4.3 Energy output structure

The detonation wave propagates to the interface between the explosive and water when a charge explodes underwater. A part of the explosion energy spreads out in the form of the initial shock wave, and the remaining energy is retained in the detonation products. Thus, the subsequent bubble pulsation is maintained (bubble energy E_b). The energy losses in the propagation of the shock wave cause the shock wave energy to vary at different measuring points. The lost energy is then converted to the internal energy of the water. The initial shock wave is difficult to measure at the interface between the explosive and water. Thus, the detonation heat is often considered as the sum of the initial shock wave energy (E_s^0) and E_b .

$$Q_v = E_s^0 + E_b = E_s + E_b + E_\mu \quad (6)$$

The energy loss of the shock wave E_μ can be calculated from a known detonation heat and bubble period. The energy loss of the shock wave E_μ can be also expressed as:

$$E_\mu = (\mu - 1)E_s \quad (7)$$

where μ is the loss coefficient of the shock wave energy.

Figure 3 shows that the relation between μ and P_{Cl} at different measuring points is not linear. With increasing detonation pressure, the loss coefficient initially decreases slowly, then gradually increases, and finally sharply decreases when the detonation pressure exceeds 14 GPa. Moreover, the loss coefficient decreases as the distance increases. A higher detonation pressure indicates a greater value of μ , that is, increased shock wave energy consumption in the form of heat. However, this law does not apply to RDX/AP-based aluminized

explosives. The detonation pressures of RDX/AP-based aluminized explosives are lower than those of other explosives, and the energy loss in the propagation of the shock wave is not more than that of explosives with high detonation pressures. Thus, the values of μ are smaller. Moreover, the energy released from the subsequent reaction of the Al particles and AP in the detonation products may partially supplement the shock wave energy loss in the propagation process. The proportion of shock wave energy loss can be reduced. The results show that a lower detonation pressure is not good for an underwater explosive. Therefore, optimum detonation pressure values exists and perform an important function in the energy distribution of the shock wave energy and the bubble energy.

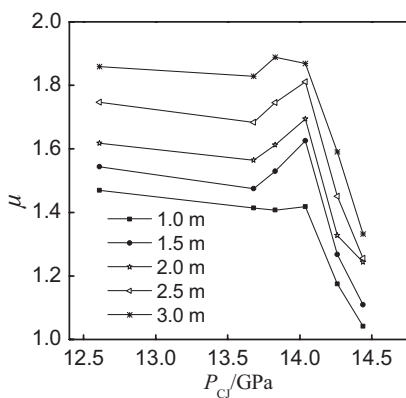


Figure 3. Relation between the loss coefficient μ and detonation pressure

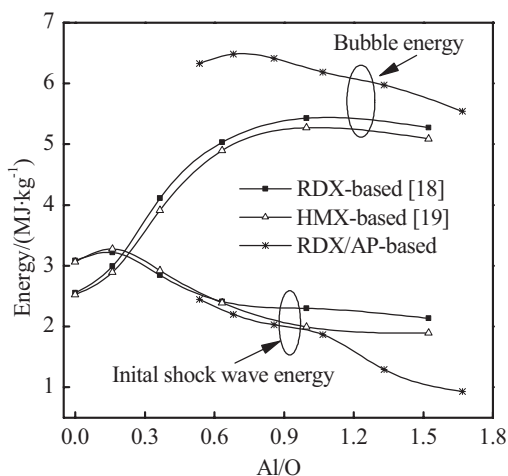


Figure 4. Relations of the shock wave energy and the bubble energy with the Al/O ratio

The relations of the initial shock wave energy and the bubble energy with the Al/O ratio for the three types of aluminized explosives are shown in Figure 4. The initial shock wave energy from the RDX/AP-based aluminized explosive is close to those of the RDX- and HMX-based aluminized explosive at Al/O ratios between 0.536 and 1.071, but sharply decreases when the Al/O ratio exceeds 1.071. The bubble energy of the RDX/AP-based aluminized explosive is consistently high, on average more than 15% compared with those of RDX- and HMX-based aluminized explosives. It presents a gradually decreasing trend with increases in the Al/O ratio. The bubble energy approaches an average of 78% of the total energy in an UNDEX test.

The different performances of the six explosive formulations after UNDEX may be related to the detonation reaction mechanism of RDX/AP-based aluminized explosives. An increasing content of Al particles significantly affects the characteristics of a non-ideal detonation, which results in a low detonation energy release rate and reaction efficiency. Thus, the detonation wave energy is reduced, which leads to a decline in the shock wave energy that is propagated into the water. A number of Al particles react with AP and release heat into the detonation product gases, which supports the bubble impulse and increases the bubble energy. Al particles continue to increase, whereas the AP content continues to decrease. The reaction between Al and AP may reach a limit. Surplus Al particles would absorb heat and result in a decline in the bubble energy. The bubble energy of RDX/AP-based aluminized explosives is larger than that of RDX-based aluminized explosives. Thus, AP is an oxygen-rich additive that improves the subsequent reactions in the detonation products.

Different explosives with varying energy output structures can be devised for UNDEX by adjusting the component proportions of Al particles and AP in the formulations. RDX/AP-based aluminized explosives have been studied in this research. The content of the Al particles and AP in the explosive should be 35% and 40%, respectively, to capitalize on the low-frequency effects of the bubble pulse and to cause extensive damage to a ship.

4.4 Similar laws of shock wave

The peak pressure, attenuation time constant, impulse and the shock wave energy flux density for the mass W of an explosive detonated underwater conform to the following forms of the respective power functions of the similarity law equation:

$$p_m = K_1(R/W^{1/3})^\alpha \quad (8)$$

$$\theta/W^{1/3} = K_2(R/W^{1/3})^\beta \quad (9)$$

$$I/W^{1/3} = K_3(R/W^{1/3})^\gamma \quad (10)$$

$$E/W^{1/3} = K_4(R/W^{1/3})^\lambda \quad (11)$$

The coefficients of the law of similarity are associated with the explosive, K_1, K_2, K_3 , and K_4 denote the magnitude of the parameter values of the UNDEX, and α, β, γ and λ represent the rate of change of the parameter values. Small absolute values cause small rates of change in the parameters.

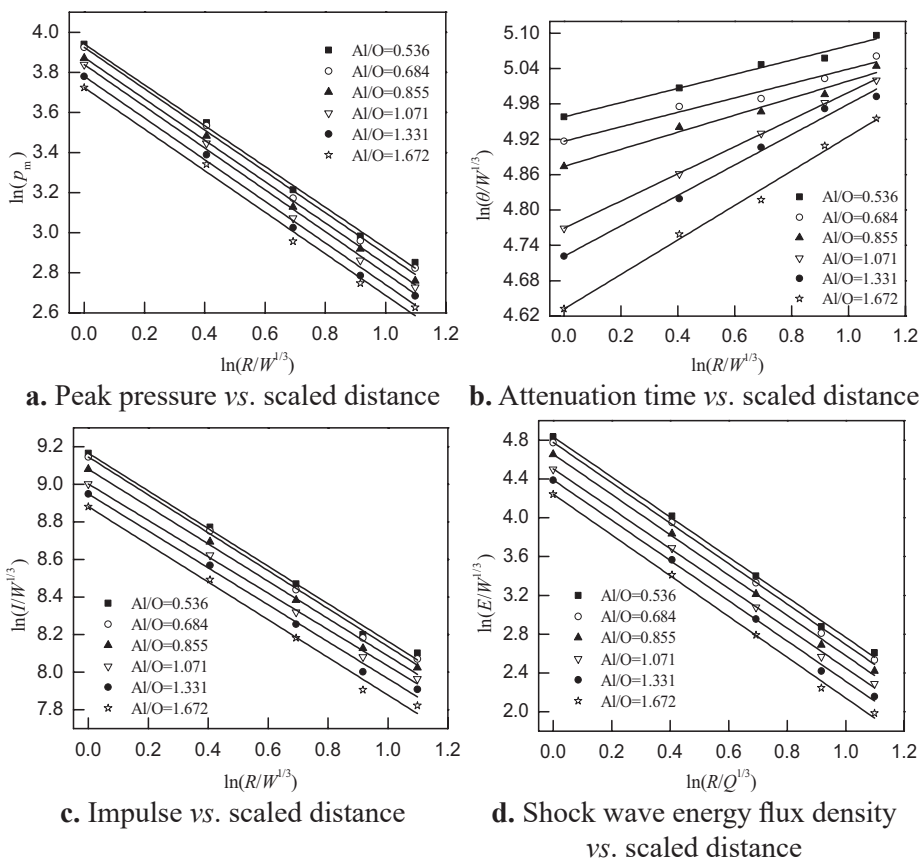


Figure 5. Parameters of the shock wave vs. scaled distance for the RDX/AP-based aluminized explosives

The measured values of p_m, θ, I and E demonstrated good linear correlations with $\ln(R/W^{1/3})$ (Figure 5). The calculated coefficients of the RDX/AP-based aluminized explosives are given in Table 3. Figure 5 and Table 3 show that $p_m, \theta,$

I and E gradually decrease with increasing Al/O ratio. θ exhibits some regularity and does not resemble that of other aluminized explosives. Increasing the Al/O ratio cannot evidently reduce the decay because of the shock wave pressure.

Table 3. Law of similarity coefficients for the RDX/AP-based aluminized explosives

Al/O	Peak pressure		Attenuation time		Impulse		Energy flux density	
	K_1 [MPa]	α	K_2 [μ s]	β	K_3 [Pa·s]	γ	K_4 [kJ·m ⁻²]	λ
0.536	51.62	-1.022	142.31	0.121	9575	-1.004	125.53	-2.057
0.684	50.81	-1.037	136.50	0.123	9390	-1.012	118.63	-2.073
0.855	48.15	-1.031	130.78	0.146	8799	-0.997	105.01	-2.066
1.071	45.66	-1.048	117.85	0.230	8132	-0.972	90.24	-2.043
1.331	43.98	-1.045	112.46	0.257	7716	-0.987	80.54	-2.065
1.672	41.62	-1.044	102.67	0.294	7209	-1.006	69.57	-2.090

4.5 Simulation of the bubble

Considering the theory of UNDEX, an arbitrary partitioning of the UNDEX bubble phenomenology into shockwave and oscillation phases defines their time of connection. Figure 6 shows that the radius vs. time and the velocity vs. time curves of the initial bubbles for a 1 kg RDX/AP-based aluminized explosive charge detonated at a depth of 4.7 m, can be derived in accordance with the volume-acceleration model using the law of similarity coefficients of the shock wave [20]. The radius of the bubble increases and the radial velocity abruptly increases within 0.06 ms, before gradually decreasing with time. The parameters of the initial bubble are not significantly different. The radial velocity changes slowly when $t > 0.6$ ms.

To study the bubble pulsation of UNDEX for the RDX/AP-base aluminized explosives, $t = 1.0$ ms was considered as the initial bubble formation time, and the nonlinear MSC.DYTRA finite element (FE) software was used for the simulation. The dimensions of the water region were set as $10.0 \times 10.0 \times 10.0$ m³ and those of the air region as $10.0 \times 2.0 \times 10.0$ m³ using the FE model. The fluid elements in the FE model were represented using hexahedral elements, and the total number of elements used in this simulation was 640,000. Two subroutines were developed to define the initial and boundary conditions in the fluid field [19].

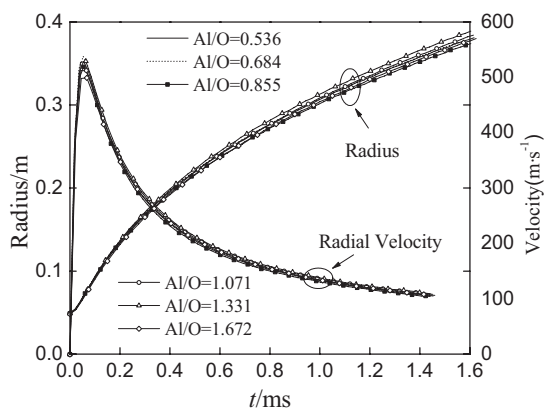


Figure 6. Time history of the radius and velocity of the bubble at a depth of 4.7 m

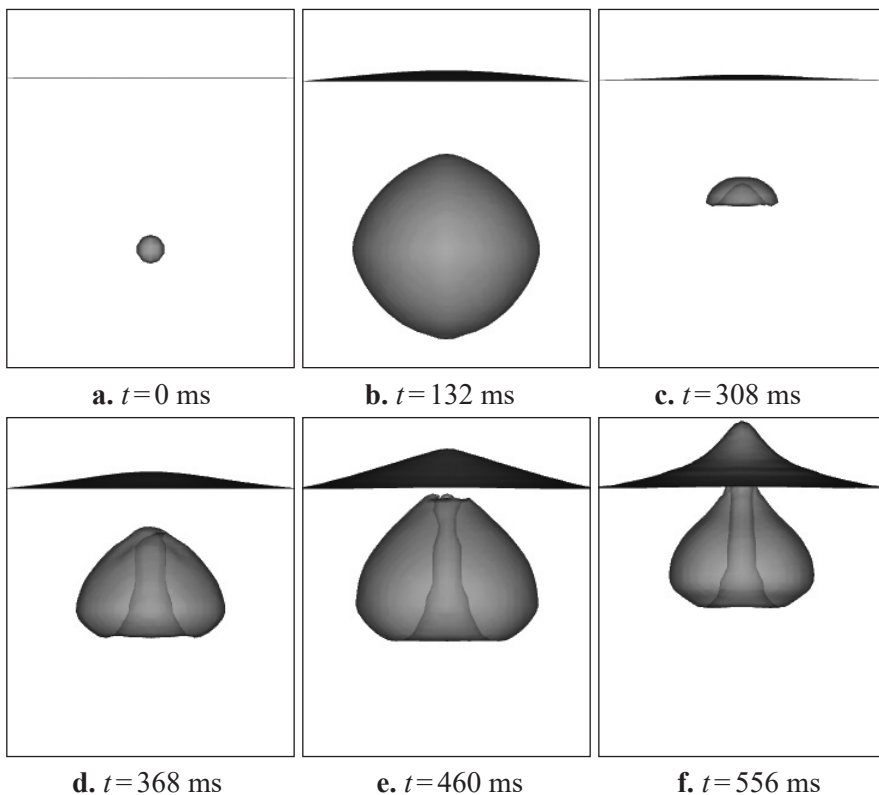


Figure 7. Typical evolution of the bubble for the formulation 20RDX/30Al/45AP/5 binder at a depth of 4.7 m; (a) $t=0$ ms, (b) $t=132$ ms, (c) $t=308$ ms, (d) $t=368$ ms, (e) $t=460$ ms, (f) $t=556$ ms

Figure 7 presents the bubble's entire evolution in two periods. The calculated motion agrees closely with that in a previous small-dose experiment during the expansion and early collapse [21]. The detonation depth was greater than the maximum bubble radius. Thus, only a small spray dome is formed on the free surface in the first period shown for the bubble expansion (Figures 7a-7c). The position of the bubble is almost constant during its expansion, but the bubble rises more distinctly when the bubble is becoming smaller (Figure 7c). The collapse unfolds when the bubble contracts to its minimum size. The bubble continues to expand and the collapse evolves into a liquid jet. The entire process of bubble pulsation, which includes the collapse and formation of the liquid jet, can be clearly and directly observed in the numerical simulation.

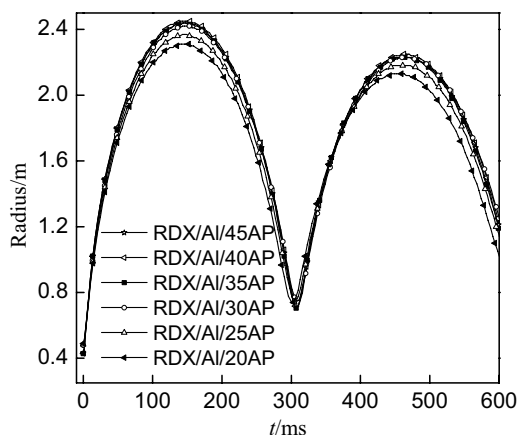


Figure 8. Radius vs. time history curves for 1.0 kg explosive charges of different compositions at a depth of 4.7 m

Figure 8 shows that the radius of the bubble as a function of time in the numerical results for the six formulations of the RDX/AP-based aluminized explosive. Table 4 shows the experimental, numerical, and empirical results for the period and maximum radius of the bubbles. The numerical results of the period of the bubble and the empirical results agree well with the experimental data, with an average error of approximately 8.6%. No experiment results are available for the bubble radius. The empirical and numerical results of the maximum radius of the bubble were 2.63 m and 2.45 m, respectively, when the Al/O ratio was 0.684. The average error was less than 8%. Error analysis showed that the initial bubble parameters used in the model may encounter some problems, or that the volume-acceleration model may not be suitable for RDX/AP-based aluminized explosives.

Table 4. Bubble parameters of the RDX/AP-based aluminized explosives

Al/O	Bubble period			Maximum radius of bubble		
	Exp. [ms]	FEA [ms]	Error [%]	Eq.(1) [m]	FEA [m]	Error [%]
0.536	338.3	307	-9.3	2.63	2.44	-7.4
0.684	340.9	309	-9.4	2.63	2.45	-6.7
0.855	339.7	307	-9.6	2.60	2.44	-6.2
1.071	335.7	308	-8.3	2.56	2.42	-5.5
1.331	332.0	304	-8.4	2.47	2.37	-4.2
1.672	324.1	303	-6.5	2.38	2.31	-3.0

5 Conclusions

The UNDEX performance of RDX/AP-based aluminized explosives was studied by explosion in a water pool. Six formulations of the explosive were investigated, all of which contained RDX, AP, Al particles, wax and graphite, with Al content from 30% to 55% and AP content from 45% to 20%. The results showed that the value of θ for the RDX/AP-based aluminized explosives decreases linearly with increases in the Al/O ratio, which is different from that of RDX- and HMX-based aluminized explosives. The logarithmic values of p_m , θ , I and E of the shock wave show excellent linearity with the scaled distance. The RDX/AP-based aluminized explosives in the present study exhibit higher E_b values, on average of more than 15%, compared with those of RDX- and HMX-based aluminized explosives. Moreover, E_b approaches an average of 78% of the total energy in the UNDEX test. E_b does not follow a direct relationship between detonation heat and bubble energy. These different UNDEX performances indicate that the detonation reaction mechanism of RDX/AP-based aluminized explosives differs from that of RDX-based aluminized explosives. AP provides more oxygen and enhances the combustion efficiency of the Al particles, which causes the release of more energy in the detonation products. The entire evolution of the bubbles was well-simulated by the MSC.DYTRAN software. The bubble radius history showed that the numerical period and the maximum radius of the bubble were smaller than the experimental and empirical results, respectively. The errors indicate that the volume-acceleration model may not be suitable for studying RDX/AP-based aluminized explosives.

Acknowledgements

The authors would like to express their gratitude to Dr. Xiaojun Feng and Dr. Hao Wang, whose efforts were essential in the detonation experiments. This

research was supported by the National Natural Science Fund of China (Project No. 11502021) and NSAF (Grant No. U1530147).

References

- [1] Cole, R. H. *Underwater Explosions*. Princeton University Press, New Jersey, **1948**; ISBN 9780691069227.
- [2] Gogulya, M. F.; Makhov M. N.; Dolgoborodov, A. Y.; Brazhnikov, M. A.; Arkhipov, V. I.; Shchetinin V. G. Mechanical Sensitivity and Detonation Parameters of Aluminized Explosives. *Combust. Explos. Shock Waves (Engl. Transl.)* **2004**, *40*(4): 445-457.
- [3] Mader, C. L. *Numerical Modeling of Detonations*. Berkeley, University of California Press, **1979**.
- [4] Hobbs, M. L.; Baer, M. R. Calibrating the BKW-EOS with a Large Product Species Database and Measured C-J Properties. *Proc. 10th (Int.) Symp. Detonation*, Boston, MA, USA, **1993**, 409-418.
- [5] Keshavarz, M. H.; Teimuri, M. R.; Esmail, P. K.; Shokrollahi, A.; Zali, A.; Yousefi, M. H. Determination of Performance of Non-ideal Aluminized Explosives. *J. Hazard. Mater. A* **2006**, *137*: 83-87.
- [6] Keshavarz, M. H.; Motamedoshariati, R. H.; Moghayadnia, R.; Nazari, H. R.; Azarniamehraban, J. A New Computer Code to Evaluate Detonation Performance of High Explosives and Their Thermochemical Properties, Part I. *J. Hazard. Mater.* **2009**, *172*: 1218-1228.
- [7] Pei, H. B.; Nie, J. X.; Jiao, Q. J. Study on the Detonation Parameters of Aluminized Explosives Based on a Disequilibrium Multiphase Model. *Cent. Eur. J. Energ. Mater.* **2014**, *11*(4): 491-500.
- [8] Keshavarz, M. H.; Zamani, A. A Simple and Reliable Method for Predicting the Detonation Velocity of CHNOFCl and Aluminized Explosives. *Cent. Eur. J. Energ. Mater.* **2015**, *12*(1): 13-33.
- [9] Cichra, D. A.; Doherty, R. M. Estimation of Performance of Underwater Explosives. *Proc. 10th (Int.) Symp. Detonation*, Portland, OR, USA, **1989**, 33-39.
- [10] Swisdak, M. M. *Explosion Effects and Properties. Part II. Explosion Effects in Water*. Report No. ADA056694, U.S. Naval Surface Weapons Center White Oak Lab, Silver Spring, MD, **1978**.
- [11] Stromsoe, E.; Eriksen, S. Performance of High Explosives in Underwater Applications. Part 2: Aluminized Explosives. *Propellants Explos. Pyrotech.* **1990**, *15*: 52-53.
- [12] Adapaka, S. K.; Vepakomma, B. R.; Rabindra, K. S.; Alapati, S. R. Evaluation of Plastic Bonded Explosive (PBX) Formulations Based on RDX, Aluminum, and HTPB for Underwater Applications. *Propellants Explos. Pyrotech.* **2010**, *35*: 359-364.

- [13] Wang, L. Q.; Wang, N. F.; Zhang, L. Study on Key Factors Affecting Energy Output of Emulsion Explosives in Underwater Explosion. *Propellants Explos. Pyrotech.* **2012**, *37*: 83-92.
- [14] Bocksteiner, G. *Evaluation of Underwater Explosion Performance of PBXW-115(AUST)*. Report No. DSTO-TR-0279, Australia, Weapon Systems Division Aeronautical and Maritime Research Laboratory, VIC, **1996**.
- [15] Lu, J. P.; Kennedy, D. L. *Modelling of PBXW-115 Using Kinetic CHEETAH and the DYNA Codes*. Report No. DSTO-TR-1496, Australia, Weapons Systems Division Systems Sciences Laboratory, SA, **2003**.
- [16] Satyavratana, P. V.; Vedam, R. Some Aspects of Underwater Testing Method. *Propellants Explos. Pyrotech.* **1980**, *5*: 62-66.
- [17] Gaspin, J. B. *Depth Scaling of Underwater Explosion Source Levels*. Report No. ADA020473, U.S. Naval Surface Warfare Center, MD, **1975**.
- [18] Xiang, D. L.; Rong, J. L.; Li, J.; Feng, X. J.; Wang, H. The Effect of Al/O Ratio on Detonation Performance and Underwater Explosion of RDX-based Aluminized Explosive (in Chinese), *ACTA Armamentarii* **2013**, *34*(1): 1296-1301.
- [19] Xiang, D. L.; Rong, J. L.; Li, J. Effect of Al/O Ratio on the Detonation Performance and Underwater Explosion of HMX-based Aluminized Explosives. *Propellants Explos. Pyrotech.* **2014**, *39*: 65-73.
- [20] Li, J.; Rong, J. L. Bubble and Free Surface Dynamics in Shallow Underwater Explosion. *Ocean Eng.* **2011**, *38*: 1861-1868.
- [21] Klaseboer, E.; Hung, K. C.; Wang, C.; Wang, C. W.; Khoo, B. C.; Boyce, P.; Debono, S.; Charlier, H. Experimental and Numerical Investigation of the Dynamics of an Underwater Explosion Bubble Near a Resilient/Rigid Structure. *J. Fluid Mech.* **2005**, *537*: 387-413.